Pharmaceutical Development and Technology

ISSN: 1083-7450 (Print) 1097-9867 (Online) Journal homepage: http://www.tandfonline.com/loi/iphd20

PLGA-PEG-RA-Based Polymeric Micelles for Tumor Targeted Delivery of Irinotecan

Jaber Emami, Parnian Maghzi, Farshid Hasanzadeh, Hojjat Sadeghi, Mina Mirian & Mahboubeh Rostami

To cite this article: Jaber Emami, Parnian Maghzi, Farshid Hasanzadeh, Hojjat Sadeghi, Mina Mirian & Mahboubeh Rostami (2017): PLGA-PEG-RA-Based Polymeric Micelles for Tumor Targeted Delivery of Irinotecan, Pharmaceutical Development and Technology, DOI: 10.1080/10837450.2017.1340950

To link to this article: http://dx.doi.org/10.1080/10837450.2017.1340950

Accepted author version posted online: 13 Jun 2017.

Author Information

Professor Jaber Emami (Corresponding Author)
Email: Emami@pharm.mui.ac.ir
Affiliation 1:
Dept. of Pharmaceutics, School of Pharmacy and Pharmaceutical Sciences, Isfahan University of Medical Sciences, Isfahan, Iran (the Islamic Republic of)

Dr Parnian Maghzi
Email: parnian_maghzi1368@yahoo.com
Affiliation 1:
Dept. of Pharmaceutics, School of Pharmacy and Pharmaceutical Sciences, Isfahan University of Medical Sciences, Isfahan, Iran (the Islamic Republic of)

Professor Farshid Hasanzadeh
Email: hasanzadeh@pharm.mui.ac.ir
Affiliation 1:
Dept of Medicinal Chemistry, School of Pharmacy, Isfahan University of Medical Sciences, Isfahan, Iran (the Islamic Republic of)

Professor Hojjat Sadeghi
Email: sadeghi@pharm.mui.ac.ir
Affiliation 1:
Department of Biotechnology, School of Pharmacy and Pharmaceutical Science, Isfahan University of Medical Sciences,, Isfahan, Iran, Islamic Republic of
---
Mrs Mina Mirian
Email: mirian@pharm.mui.ac.ir
Affiliation 1:
Department of Biotechnology, School of Pharmacy and Pharmaceutical Science, Isfahan University of Medical Sciences,, Isfahan, Iran, Islamic Republic of
---
Dr Mahboubeh Rostami
Email: rostami@pharm.mui.ac.ir
Affiliation 1:
Dept of Medicinal Chemistry, School of Pharmacy, Isfahan University of Medical Sciences, Isfahan, Iran (the Islamic Republic of)

Keywords

Irinotecan
PLGA
PEG
Retinoic acid
Micelle,
HepG2, HT-29

Abstract

To develop an effective therapeutic treatment, the potential of poly (lactic-co-glycolic acid)-polyethylene glycol-retinoic acid (PLGA-PEG-RA) polymeric micelles for targeted delivery of irinotecan to hepatocellular carcinoma (HepG2) and colorectal cancer cell lines (HT-29) was evaluated. PLGA-PEG-RA was synthesized by amide reaction of PLGA with NH2–PEG–NH_2 and then PLGA-PEG-NH_2 with RA and confirmed by FTIR and ^{1}H NMR spectroscopy. Irinotecan-loaded nanomicelles were prepared using thin-film hydration method and the impact of various formulation variables on their particle size (PS), polydispersity index (PDI), zeta potential (ZP), entrapment efficiency (EE), and mean release time (MRT) were assessed using a Taguchi design. TEM was used to observe morphology of the nanomicelles and the CMC was determined by fluorescence spectroscopy. Adopted PLGA-PEG-RA nanomicelle exhibited PS of 160 ± 9.13 nm, PDI of 0.20 ± .05, ZP of -24.9 ± 4.03 mV, EE of 83.9 ± 3.61 %, MRT of 3.28 ± 0.35 h, and CMC value of 25.7 μg/mL. Cytotoxicity of the targeted nanomicelles on HepG2 and HT-29 cell lines was significantly higher than that of non-targeted nanomicelles and the free drug. These results suggest that PLGA-PEG-RA nanomicelles could be an efficient delivery system of irinotecan for targeted therapy of colorectal cancer and hepatocellular carcinoma.

Introduction

One of the major concerns with conventional chemotherapy use is systemic toxicities. Besides the beneficial characteristics of destroying cancer cells, anticancer agents also destroy healthy tissue resulting in systemic toxicity[1,2]. One effective approach to cancer treatment is to prolong the exposure of tumor cells to cytotoxic drugs while reducing the exposure of healthy normal cells to such agents. Drug-loaded nanoparticles of biodegradable polymers have great potential

to provide an ideal solution for most major problems encountered in chemotherapy[3]. To increase selectivity of these drug-loaded nanoparticle delivery systems, various targeting moieties and ligands with passive and active actions have been immobilized on the surface of these nanoparticles[4].

Passive targeting is achieved by modification of nanoparticle surface with various hydrophilic linkers such as polyethylene glycol (PEG). This prevents the uptake of nanoparticles by reticuloendothelial system (RES) and increases their circulation time in the blood stream[5]. The water-soluble PEG blocks, with a molecular weight from 1 to 15 kDa, are also considered as the most suitable hydrophilic corona-forming blocks[6]. Various preclinical and clinical studies have shown the potential use of PEG conjugated polymeric micelles with different hydrophobic blocks such as PLGA[7-9] in anticancer therapy. It is noteworthy that five different PEGylated polymeric micellar formulations of chemotherapeutic agents including paclitaxel, SN-38, epirubicin and cisplatin are currently under clinical trials as potential anticancer treatment options[10].

Long-circulating PEGylated liposomes have been developed. Sadzuka *et al.*[11] reported that tumor accumulation and antitumor activity of irinotecan was increased and its side effects were reduced when PEG-modified liposomes were used. A temperature sensitive doxorubicin-loaded PEGylated liposome has been developed to release encapsulated doxorubicin at elevated tissue temperature[12].

On the other side, active targeting helps in delivering the drug to the site of action while minimizing its exposure to other non-targeted regions, thus increasing efficacy and reducing systemic toxicities. Utilization of some targeting ligands against tumor-cell-specific receptors

such as folic acid[13], transferrin[14], biotin and retinoic acid (RA)[15] has been reported to facilitate active targeting.

Retinoids are a class of compounds that are structurally related to vitamin A. They exhibit antiproliferative and differentiative effects, and thus are used for cancer prevention and treatment. RA has been used in combination with chemotherapeutic agents for the treatment of various cancers such as Kaposi's sarcoma, head and neck squamous cell carcinoma, ovarian carcinoma, and neuroblastoma[16]. Retinoids have been reported to reduce second malignancies in the liver and in the breast[17,18], to treat acute promyelocytic leukemia (APl)[19] when combined with other drugs , and to increase the antiproliferative and prodifferentiative effects on colon cancer cells[20,21]. The most effective clinical usage of all-trans RA in human disease was observed in the treatment of a rare leukemia, APL[22]. In humans, retinoids reversed premalignant human epithelial lesions, induced the differentiation of myeloid cells, and also helped in the prevention of lung, liver, and breast cancer[23].

The biological activities of retinoids are induced bybinding to specific nuclear receptors[24]. Retinoids including RA are transported into the cells by a membrane protein termed "stimulated by RA 6" (STRA6)[25]. Certain cancer cells such as human breast and colon tumors are known to have more than 100-fold higher STRA6 expression levels providing an excellent environment where delivery systems could be used to target cancer cells. STRA6 mRNA levels are up-regulated in mouse mammary gland tumors and human colorectal cancer[26,27]. Sun *et al.* reported that co-delivery of doxorubicin with RA markedly increased the drug concentrations both in breast tumor tissues and cancer stem cells, and thus enhanced the suppression of tumor growth while reducing the number of cancer stem cells in a synergistic manner[28].

Irinotecan, is a semisynthetic analogue of the natural alkaloid, camptothecin. Camptothecins act during the S-phase of DNA replication by stabilizing the complex formed between topoisomerase I and DNA, eventually resulting in lethal DNA breaks[29,30]. Topoisomerase I is overexpressed in several tumor types including breast, lung, and colorectal tumors[31]. Irinotecan has been clinically indicated for the treatment of colorectal cancer[32], pancreatic cancer[33], ovarian cancer[34], glioblastoma[35],and hepatocellular carcinoma[36].

The combination regime of all-trans RA and topotecan has shown that all-trans RA downregulates the protein level of RA receptor alpha (RARα), which might be the key for synergistic effects in this combination therapy. As a result, DNA damage can be induced more easily by all-trans RA[37]. RA may behave in similar manner once administered in combination with irinotecan. RA is converted to SN-38, a 100- to 1000-fold more active metabolite, in the liver and tumor. As the metabolic conversion rate of irinotecan to SN-38 is less than 10%, a large dosage of irinotecan is needed to achieve therapeutic efficacy. This, in part, could be due to the saturation of carboxylesterase by rapid release of the drug from common preparation of irinotecan[38]. Because of very poor water solubility and inability to administer sufficient quantities in an appropriate liquid dosage form and also unacceptable toxicity, SN38 was not used to treat cancer in humans. In addition, irinotecan exists in equilibrium between an active lactone form of the drug (predominant under acidic conditions) and an inactive carboxylate form (predominant at neutral or basic pH)[39]. These drug properties contribute to the marked heterogeneities in efficacy and toxicity observed clinically with irinotecan[40,41]. Hence, tumor-targeted nanocarriers represent a rational strategy to improve the pharmacokinetics and biodistribution of irinotecan, to protect the drug from premature metabolism, and to improve selectivity towards targeting cancerous tissues.

Several studies examined non-targeted liposomal formulations of irinotecan as a drug delivery carrier system since this chemotherapeutic agent can be directly loaded into liposomes owing to its moderate hydrophilicity. Although liposomes can enhance drug retention and improve therapeutic efficacy[42,43], most liposomal systems are inherently less stable and prone to leakage and fusion. Lipid nanoparticles also have some limitations such as limited drug loading capacity and drug expulsion during storage due to crystallization of lipid matrix or lipid polymorphism. Conversely, polymeric micelles might have several advantages over liposomes including their ability to penetrate tissues and control drug release without initial burst release, stability towards dilution, as well as their lower potential to induce toxicity or hypersensitivity reactions. The utilization of polymeric micelles as a drug carrier system may be limited by their particle size, stability, loading capacity and release kinetic of drugs. Importantly, these critical features can be modulated by modifying the chemical structure and physicochemical properties of the constituent copolymer[44]. In the light of the information discussed above, we sought to develop for the first time a novel targeted polymeric micelles delivery system to deliver irinotecan systemically by synthesizing PLGA-PEG-RA. This novel micellar platform may have some unique advantages for the systemic delivery of irinotecan. The PEG units form a brush-like shell, which may prevent aggregation and uptake of the micelles by the mononuclear phagocytic system[5]. Incorporation of RA molecules may serve as an efficient dual targeting ligand by improving site-specific targeting as well as anti-cancer effects through a synergistic effect with irinotecan. Physicochemical properties characterization, targeting efficacy, cytotoxicity towards hepatocellular carcinoma (HepG2) and colorectal cancer cell lines (HT-29) and also synergistic effect of RA with irinotecan on these cancer cells were evaluated in this study.

Materials and methods

Materials

PLGA (MW,12000 kDa, 50:50), PEG bis(amine) (MW, 1960), dicyclohexylcarbodiimide (DCC), N-hydroxysuccinimide (NHS), pyrene, anhydride dimethyl sulfoxide (DMSO), dehydrated pyridine and RA were purchased from Sigma Chemical Co. (St. Lois, MO). Irinotecan was procured from Arch pharmalabs (Mumbai, india). Roswell Park Memorial Institute (RPMI)-1640, fetal bovine serum (FBS), and antibiotics for cell culture were supplied by GIBCO. Hepatocellular carcinoma (HepG2) and colorectal cancer cell lines (HT-29) were obtained from Pasteur Institute of Iran (Tehran, Iran). 3-(4,5-dimethylthiazol-2-yl)-2,5-diphenyltetrazolium bromide (MTT) was obtained from Sigma-Aldrich.

Synthesis of PLGA-PEG-RA

PLGA (0.1 mmol) was activated with DCC (0.12 mmol) and NHS (0.12 mmol) in anhydrous dichloromethane (DCM) in a round-bottom flask and left to stir overnight at room temperature under nitrogen atmosphere. The solution was centrifuged at 7000 rpm for 6 min to remove the by-product dicyclohexylurea and then added dropwise to cold anhydrous THF to precipitate the activated PLGA. The product was then dried under vacuum for 24 h[45-48].

Activated PLGA (0.06 mmol) was dissolved in 8 mL anhydrous DCM. PEG bis(amine) (0.18 mmol) was also dissolved in 2 mL anhydrous DCM and added to PLGA solution in a dropwise manner. PEG bis(amine) was added in excess to suppress the formation of PLGA-PEG-PLGA triblock copolymer. The mixture was stirred gently at 400 rpm at room temperature for 6 h under nitrogen atmosphere. The solution was added to anhydrous THF to precipitate the product, which was dried under vacuum for 24 h. In the next step, RA was first activated with NHS and DCC at

a molar ratio 1:1.2:1.2 of RA//NHS/DCC in anhydrous DMSO in the presence of 0.1 mL pyridine as a catalyst under light protected condition and nitrogen gas for 24 h. Activated RA, DCC and PLGA-PEG (400 mg) were dissolved in anhydrous DMSO under the light protected condition under nitrogen atmosphere overnight. DCC was added to ensure all the RA is ready to react with PLGA-PEG. The product was transferred into a dialysis bag (Spectra/Por molecular porous membrane, MWCO 6-8 kD). The content of the bag was dialyzed against phosphate buffer (pH = 7.8), acetate buffer (pH = 6) and ethanol for 72 h with constant stirring at 600 rpm and room temperature. The product was then freeze-dried and stored in refrigerator[45-48]. The structure of PLGA-PEG-RA was confirmed by ^{1}H-NMR spectroscopy in d_6-DMSO and FTIR.

Measurement of critical micelle concentration

The critical micelles concentration (CMC) of PLGA-PEG-RA was determined by fluorescence spectrometry using pyrene as a hydrophobic fluorescence probe. Pyrene was dissolved in acetone and loaded in test tubes. After evaporation of acetone, 5 mL polymer solutions in water at various concentrations (2-500 μg/mL) were added to the tubes so that the final pyrene concentration was 6×10^{-7} M. The tubes were vortexed and stirred at 37 ºC in a bath shaker for 24 h. The fluorescence emission spectra of pyrene were recorded using spectrofluorometer (Jasco FP 750, Tokyo, Japan) with the excitation wavelength set at 360 nm. From the pyrene emission spectra, the intensity ratios of the first peak (I_1, 383 nm) to the third peak (I_3, 433 nm) were plotted against the logarithm of the polymer concentrations. Two tangents were then drawn, and the CMC value was determined from the inflection point of the two tangents[49].

Preparation of micelles

Irinotecan-loaded PLGA-PEG-RA micelle was prepared by thin-film hydration method. In brief, 2.5 or 5 mg of polymer was dissolved in 2.5 or 5 mL of acetone and 1 mg of irinotecan was

dissolved in 7.5 or 5 mL ethanol and then added to the polymeric solution in a dropwise manner. The mixture was then evaporated under vacuum at 60 ºC to form a homogenous film. The resulting film was hydrated in 10 mL phosphate buffer with pH of 7.4 or 9 at 60 ºC and stirred at 500 rpm for 2 h at 37 ºC. To reduce particle size (PS), micellar solution was then sonicated for 2 min[50]. Blank micelles were also prepared in the same manner as described above without using drug.

Experimental design and analysis

Proper planning and good experimental design procedures are essential to yield valid and objective conclusions. The preparation and optimization of nanomicelles requires conductinginitial experiments to select the optimal conditions with respect to the formulation composition and production conditions. With regard to micelles preparation method, we found that film hydration technique resulted in more efficient drug loading and smaller micellar size compared to other methods such as membrane dialysis or emulsion method. Thus, low boiling point solvents were required for this technique. Best result was achieved using ethanol and acetone in different ratios. We also assumed that adjusting aqueous external phase pH to higher values may shift the protonated drug to unionized form leading to higher micellar drug loading. Thus, two different externalphase pHs were examined. Stirring speed or sonication magnitude were found almost insignificant. Due to possible risk of drug decomposition, temperature was not studied as one of the processing variables. Therefore, in the present study, a Taguchi design with three factors of drug/polymer ratio, different solvents at various combinations, and the pH of external phase at two levels was applied to optimize the formulation. **Table 1** displays three independent variables and their levels studied in an L4 Taguchi design. All experiments were performed in triplicates. Five responses including PS, polydispersity index (PI), zeta potential

(ZP), entrapment efficiency (EE), and mean release time (MRT) were studied. The experimental results were then analyzed by the Design Expert software version 7 (Stat-Ease, Inc., Minneapolis, Minnesota, USA) to extract independently the main effects of these factors which was followed by the analysis of variance (ANOVA) to determine which factors were statistically significant[51].

Characterization of micelles

Size distribution, PDI, and ZP of the nanomicelles (1 mg/mL) were determined in saline phosphate buffer using a size/zeta potential analyzer (ZEN 3600 Malvern, U.K). A dilute dispersion of nanoparticles (20 μg/mL) was prepared in deionized distilled water and measurements were taken in specific disposable cuvettes and recorded.

Morphology of polymeric micelles

Transmission electron microscope (TEM) images (Zeiss, EM10C, 80 KV) were utilized for examining the morphology of nanoparticles. Few drops of 0.1 mg/mL drug solution containing (1:2.5) nanoparticles were placed on a Formvar carbon coated copper grid. Excess fluid was removed with a piece of filter paper and TEM images were taken after the sample was completely dried.

Entrapment efficiency and drug loading studies

For determination of EE of irinotecan in the micelles, dialysis method was used. Two mL of the drug-loaded nanomicelles were placed into the dialysis bag (cut-off 8 kDa, Float-A-Lyser®. G2, Sigma) and immersed in a plastic tube containing 10 mL phosphate-buffer saline (PBS) for 2 h with gradual gentle shaking. The concentration of irinotecan in dialysate was determined by measuring the UV absorbance at 254 nm using a UV-VIS spectrophotometer using previously

constructed calibration curve[52]. After calculating the quantity of free drug in the buffer, the drug EE and drug loading (DL) in the nanoparticles were calculated using following equations[53]:

$$EE\% = \left(\frac{initial\ amount - unloaded\ amount\ in\ dialysate}{initial\ amount} \right) \times 100$$

$$DL\% = \left(\frac{loaded\ amount\ in\ nanomicelles}{weight\ of\ nanomicelle} \right) \times 100$$

***In vitro* drug release**

The release experiment was carried out *in vitro* as follows. Five mL of drug-loaded NPs were placed in a dialysis bag (MWCO 10000 Da.) clipped at both the ends and dialyzed against 50 mL of PBS (pH 7.4) with agitation rate at 100 rpm at 37 ºC. At predefined intervals, 1 mL of receiving buffer solution was withdrawn and irinotecan content was determined at 254 nm by a UV spectrophotometer. At each withdrawal, the dialysis medium was replaced with 1 mL of fresh medium. MRT was calculated using equation below.

$$MRT = \frac{\sum_{i=1}^{n} t_{mid} \times \Delta M_i}{\sum_{i=1}^{n} \Delta M_i}$$

where, i is the sampling number, n is the number of last dissolution sample, t_{mid} the time at midpoint between t_i and t_{i-1} (calculated as $(t_i+t_{i-1})/2$) and ΔM_i is the additional amount of drug dissolved between t_i and t_{i-1}[54].

In order to evaluate the drug release kinetics and mechanism, the release profiles were fitted into zero-order ($W_R = K_0\ t \pm b$), first-order ($Ln\ W_L = Ln\ W_0 - K_1 t$), Higuchi ($W_R = K_H t_{1/2}$) kinetics, and Korsmeyer-Peppas equation ($Log\ (W_R/W_0) = Log\ k + n\ Log\ t$); where, W_R is the amount of

drug released at the sampling time t, W_L is the amount of drug remained within the nanomicelles at the sampling time t, W_0 is the initial amount of drug within the system, K is the drug release rate constant. In model Korsmeyer-Peppas, the value of n characterizes the release mechanism of the drug from nanomicelles[54].

***In vitro* cell toxicity assay**

HT-29 and HepG2 cell lines were obtained from Pasteur Institute of Iran (Tehran, Iran). Cells were grown at 37 ºC in humidified atmosphere containing 5% CO_2 in RPMI 1640 medium supplemented with 10% FBS, 100 IU/mL penicillin, and 100 IU/mL streptomycin.

Cytotoxicity of irinotecan solution, blank, non-targeted, and targeted irinotecan-loaded nanomicelles were assessed against HT-29 and HepG2 cell lines using MTT assay. The cells were seeded at density 4×10^4 cells/mL in a 96-well culture plate (SPL Lifescience, Gyeonggi-Do, Korea). When the cell confluence reached 75 %, the cells were incubated with samples for 72 h at the equivalent irinotecan concentrations of 1 to 8 µg/mL. After incubation, 20 µL of MTT solution (5 mg/mL in 0.02 M PBS) was added to each well and the plate was incubated for another 4 h. Subsequently, unreacted MTT and medium was removed and the formazan crystals in cells were dissolved in 180 µL of DMSO. The absorbance was measured at 570 nm using an enzyme-linked immunosorbent assay plate reader (Stat Fax-2100; Awareness Technology Inc., Palm City, FL). Untreated cells were taken as the negative control and the blank culture medium was used as the blank control. Cell viability for each sample was calculated using the following equation[55].

$$Cell\ \text{survival}\% = \left(\frac{mean\ of\ each\ group - mean\ of\ blank}{mean\ of\ negative\ control - mean\ of\ blank} \right) \times 100$$

Statistical analysis

Data were expressed as means of three separate experiments and were compared by one way ANOVA for multiple groups. A *P*-value < 0.05 was considered statistically significant in all cases.

Results

Use of irinotecan, as an antineoplastic agent, in PLGA-PEG-RA conjugate, helps in delivery of the toxic anticancer agents to the site of action and minimizes its exposure to non-targeted regions. Successful synthesis of PLGA-PEG-RA was carried out in consecutive four-step reactions as depicted in **Fig. 1** and was confirmed by ^{1}H-NMR and FTIR.

Fig. 1

Chemical shifts (δ) were expressed in parts per million (ppm) relative to the NMR solvent signal (d_6-DMSO) with tetramethylsilane as an internal standard. **Fig. 2** and **Fig. 3** demonstrate various proton peaks associated with PLGA-PEG-RA polymer.

Fig. 2 **Fig. 3**

PLGA is a copolymer of poly lactic acid (PLA) and poly glycolic acid (PGA). In **Fig. 2A**, Peak (a) in PLA moiety of the molecule is a multiplet peak in 5.15-5.28 ppm with a little chemical shift is appeared in 5.19-5.29 ppm in the final product (**Fig. 3B**). This could be due to the chemical bonding between the carboxyl group of PLGA and amine group of PEG bis(amine). Peaks (a") at 4.12 ppm in the final product spectrum (**Fig. 3B**) and (b") at 3.00-3.06 ppm as a multiplet peak in primary PEG (**Fig. 2B**) shifting to downfield regions in the final product also confirms the successful chemical bonding. Distinctive peaks of RA are denominated from (a') to

(o'), respectively (**Fig. 3A**). Peaks assigned as (a') pertaining to carboxyl group of RA are shifted in an appropriate region in the final product. Because of the chemical bonding between the end amine group of PEG bis(amine) and carboxyl group of RA, the most important peak (g') is shifted from 5.6 ppm in the PEG spectrum (**Fig. 2B**) to 5.8 in the spectrum of final product (**Fig. 3B**). More importantly, the peak corresponding to the carboxyl group of RA appeared at 12 ppm in the spectrum of RA (**Fig. 3A**) is absent in the spectrum of final product. NMR spectrum of physical mixture (**Fig. 4**) does not show any of these chemical shifts. Also signal at 12 ppm corresponding to –COOH of RA exists in physical mixture spectrum. These data collectively demonstrates successful synthesis of expected PLGA-PEG-RA polymer[56].

Fig. 4

Further elucidation was carried out using FTIR spectra of PLGA, PEG bis(amine), RA and PLGA-PEG-RA (**Fig. 5a-d**). Absorption band at 3355 cm^{-1} (**Fig. 5a**) is assigned to amine group of PEG bis(amine). In FTIR spectrum of PLGA (**Fig. 5b**), the signal related to the stretching vibration of the carbonyl group of repeating units of glycolic and lactic acid was observed at 1757 cm^{-1}. Also, the absorption band at 1679 and 2931 cm^{-1} represent respectively the carbonyl and hydroxyl groups in RA structure (**Fig. 5c**). The typical absorption band at 1756 cm^{-1} confirmed the formation of new amide bonds in the product and the successful synthesis of PLGA-PEG-RA (**Fig. 5d**)[57].

Fig. 5

The CMC of nanomicelles

To determine the critical micelle concentration of PLGA-PEG-RA, fluorescence study was performed using pyrene as the hydrophobic probe. Below the CMC, pyrene is solubilized in

water, a medium of high polarity. Once micelles are formed, pyrene partitions preferentially towards the hydrophobic domain afforded by micellar core and thus experiences a non-polar environment. The value of CMC was obtained from the plot of fluorescence intensity of the I_1/I_3 ratio from emission spectra against pyrene concentration. The CMC value of PLGA-PEG-RA copolymer was found to be 25.7 μg/ml.

Micelle characterization

Nanomicelles were successfully prepared by thin-film hydration method. Some formulation variables such as drug/polymer ratio, ethanol/acetone and pH of buffer were used to optimize the formulation. **Table 1** shows the effect of these variables on PS, PDI, ZP, EE, and MRT of irinotecan-containing micelles. PS and PDI of all formulations were mostly less than 200 nm and 0.3, respectively. ZP of the produced nanoparticles was found to be negative and absolute value of ZP in most formulation was above 20 mV. Contribution percent of different effective factors on the PS, PDI, ZP, EE, and MRT of nanomicelles loaded with irinotecan are shown in **Fig. 6.**

Table 1 **Fig. 6**

PLGA-PEG-RA nanomicelles were further characterized for morphology by TEM (**Fig. 7**). The nanoparticles were discrete, spherical with smooth surface and the scale bar of the image confirms the size of the micelles. Physical characteristics of irinotecan-loaded-PLGA-PEG-RA nanomicelles are tabulated in **Table 1**. The EE for all formulations was greater than 80% and did not change significantly by changing formulation variables. DL%, on the other hand, was mostly affected by the amount of polymer used in each formulation ranging from 15.6% for formulation F1 to 31.2% for formulation F2. Nanomicelles were further characterized for *in vitro* drug release. **Fig. 8** shows that the drug release from nanomicelles in the first 4 h was faster due to hydrophilic properties of the drug. Subsequently the release rate was decreased slowly. Also it

was observed that MRT is more affected by solvent ratio. Irinotecan release kinetics from the prepared nanoparticles using Taguchi designs indicated that the release kinetics of all formulations followed Higuchi kinetics. The release mechanism was determined based on the values (**Table 1**) calculated for n through the Peppas equation.

Fig. 7 **Fig. 8**

Optimized formulation

Computer optimization process and a desirability function determined the effect of the levels of independent variables on the responses. All responses were fitted to the linear model. The constraints of PS were 140 to 210 nm with targeting the PS in to lowest, for ZP was −18 to −28 mV, while the target was the highest value of ZP, for the EE the constraint was 75 to 87% with the target in range 79-84 values, and for release percent the target was considered in the range of the measured values. Accordingly, the predicted optimized formulation by the software would be fit to F2. To confirm the predicted model, the optimized formulation was prepared, and the observed responses were measured and listed in **Table 2**. The acceptable agreement between the observed values and the values predicted by the software and the negligible error percent confirm the validation and reliability of our method as well as its adequate precision for the prediction of optimized conditions in the domain of levels chosen for the independent variables.

Table 2.

***In vitro* cytotoxicity studies**

The cytotoxicity of free irinotecan, blank, non-targeted irinotecan-loaded PLGA–PEG, and irinotecan-loaded PLGA–PEG-RA nanomicelles were investigated against HT-29 and HepG2 cell lines. As shown in **Fig. 9**, blank micelles did not show any measurable toxicity on both cell

lines indicating that PLGA-PEG-RA could be considered a safe drug delivery carrier for the delivery of irinotecan to the cancerous cells. Cell toxicity of irinotecan and irinotecan-loaded nanomicelles were enhanced in a drug concentration dependent manner. Considerable toxicity was observed when the cells were exposed to higher concentrations of irinotecan. Non-targeted irinotecan-loaded PLGA–PEG nanomicelles showed greater ($P < 0.05$) cytotoxicity in both cell lines as compared to that of free irinotecan. The cell toxicity of irinotecan-loaded targeted PLGA–PEG-RA nanomicelles, however, was significantly greater than free irinotecan and non-targeted irinotecan-loaded PLGA–PEG nanomicelles.

The 50% inhibitory concentration (IC_{50}) values of free irinotecan and prepared nanomicelles are shown in **Table 3**. IC_{50} values of drug-loaded PLGA–PEG and drug-loaded PLGA–PEG-RA nanomicelles were significantly ($P < 0.05$) lower than those of free drug in both cell lines. Irinotecan-loaded PLGA–PEG-RA nanomicelles exhibited lowest IC_{50} values for both cell lines as compared to free irinotecan and non-targeted nanomicelles. PLGA–PEG–RA micelles exhibited less toxicity against HepG2 cells than HT-29 cells.

Fig. 9 **Table 3**

Discussion

Effective delivery and targeting of anticancer agents at the tumor site and cancerous cells has been one of the forefront of projects in cancer chemotherapy. Site specific targeting of nanoparticulate and colloidal drug delivery systems could improve the specificity, provide more effective therapy, reduce the toxicity and maintain blood circulation of drug-loaded nanoparticles[58]. In recent years, a number of nanoparticle-based therapeutic systems have been developed for the treatment of a variety of cancers. In the current study, PLGA-PEG-RA nanomicelles were prepared as a micellar system for the delivery of the chemotherapeutic agent

irinotecan to tumor cells. Polyethylene glycol has been extensively employed as a shell forming polymer to prevent the uptake of nanocarriers by macrophages and also to inhibit the aggregation of nanoparticles[59]. RA serves as a targeting moiety to the STRA6-overexpressed cancer cell lines and also to impart optimum physical characteristics to the PLGA-PEG-RA molecule to facilitate formation of micelles. Successful preparation of PLGA-PEG-RA conjugates was confirmed by ^{1}H-NMR and FTIR spectroscopy.

To determine the critical micelle concentration of PLGA-PEG-RA the fluorescence study was performed using pyrene as the hydrophobic probe. Fig. 6 shows that at low concentration of PLGA-PEG-RA there were small or negligible changes in total fluorescence intensity and the ratio of the first peak to the third peak (I_{383} /I_{433}) in the emission spectra of pyrene remained constant. By increasing the concentration of PLGA-PEG-RA to achieve CMC, the incorporation of pyrene into the micelles led to a significant increase in total fluorescence intensity. The intensity of the third peak in the emission spectra of pyrene was increased in a non-proportional fashion to the first peak. Fig.7 shows the variation of fluorescence intensity ratio (I_{383}/I_{433}) against logarithm of PLGA-PEG-RA concentrations. The CMC value of PLGA-PEG-RA copolymer was found to be 25.7 µg/ml in deionized water indicating that micelles could maintain their stability after dilution in the blood circulation. The magnitude of the CMC values of PLGA-PEG copolymer varies between 5 to 20 µg/mL depending on the length of the copolymer[60]. Higher CMC values observed in our study might be related to an increase in the lipophilicity of PLGA-PEG-RA conjugate resulting from RA conjugation.

Thin-film hydration method was used to prepare irinotecan-loaded nanomicelles. The polymeric solution of polymers was evaporated by rotary evaporator at 60 ºC to form a homogenous film. The resulting film was dispersed in phosphate buffer (with different pH) and then vortexed and

stirred overnight at 37 ºC. **Table 1** shows the effect of different variables on PS, PDI, EE and MRT of irinotecan. In general, the size of nanoparticles affects their *in vivo* bio distribution. The cut-off size of tumor vasculature is about 200–700 nm[61]. The average size of the micelles developed in the present study was smaller than 200 nm rendering them acceptable for targeted delivery of anticancer agents in chemotherapy. The micelles showed a unimodal size distribution with relatively low (0.26–0.36) PDI implying a narrow size distribution among all formulations. The size of drug-loaded nanoparticles was slightly higher than that of drug-free ones due to the incorporation of drug in the micelles core. As indicated in **Fig. 6**, the most important factor ($P < 0.05$) that affects particle size is drug/polymer ratio. Additionally, the size of the drug-loaded micelles was significantly affected by the feeding ratio in the range of 1:2.5 to 1: 5. Increasing polymer content of the polymer micellar self-aggregates resulted in bigger nanoparticles.

ZP is often a key factor to understand the stability of colloidal dispersion. A higher zeta potential value may provide a repelling force between the micelles indicating better stability of this colloidal system[62]. As shown in **Table 1**, the absolute value of ZP in the majority of formulation was above 20 mV. This demonstrates that the nanoparticles dispersion obtained by rotary evaporation method in this study is a physically stable system. It was observed that all nanomicelles exhibited a negative ZP (**Table 1**), which may be attributed to the presence of ionized carboxyl groups of PLGA segments on the surface of nanoparticles. Though pH had greater effect on the ZP than other two variables, the relatively steady ZP values observed suggested that the stability of this micelle system was unaffected by the change in experimental conditions studied.

TEM was used to visualize directly the size and morphology of drug-loaded micelles (**Fig. 7**). Smooth sphere morphology and a uniform size distribution were observed for irinotecan-loaded micelles. As the PS and surface chemistry determine the fate of the micelles in blood circulation, the polymeric micelles prepared in this study may be appropriate for *in vivo* applications in cancer therapy.

Our nanomicelle delivery system proved efficacy as depicted by the ability of micellesto trap irinotecan with a very high efficiency. The EE for all formulations was greater than 80% and did not undergo significant changes from one formulation to another. This finding implied that the polymer micellar self-aggregates provided sufficient molecular space within the core itself and thus could achieve a high degree of drug loading[63]. To increase EE, the pH of the external phase was adjusted to 9 to form the base form of irinotecan to decrease its solubility in water phase in order to increase EE. Unexpectedly, the EE was decreased at this pH. Irinotecan exist in an active lactone form and an inactive hydroxyl-acid anion form. A pH-dependent equilibrium exists between the two forms such that a low pH (acidic conditions) promotes the formation of the active lactone, whilst a more basic pH forces the equilibrium to shift to form the inactive hydroxyl-acid anion form[64]. This unexpected reduction in EE, might be related to inactivation of lactone ring in irinotecan structure. Polymer contents to drug weight ratio was an effective factor on EE in nanomicelles. The increase in polymer concentration was accompanied with more entrapment of drug in the nanomicelles. When the initial feeding ratio of irinotecan to polymer increased from 1:2.5 to 1:5 (w/w), the amount of irinotecan introduced into the micelles increased[51]. Increased PLGA concentration led to increasing the PS, and the slight increase in PS yielded better drug entrapment.

In vitro drug release study is a prerequisite for evaluating the *in vivo* performance of a drug delivery system. This is because the *in vitro* drug release profile provides the most sensitive and reliable information for *in vivo* evaluation that helps in ascertaining the future behavior of the designed formulation with regard to its drug release pattern and the time duration of its action in a biological system. **Fig. 8** shows that the drug release from nanomicelles in the first 4 h is fast due to hydrophilic properties of drug and interfacial drug loading. Subsequently the release rate was decreased slowly. As shown in **Fig. 6**, MRT is more affected by solvent ratio of ethanol to acetone than other factors evaluated during the preparation process of the nanoparticles. The release rate became faster when equal volumes of ethanol and acetone were used. Formulations containing greater amount of polymer exhibited nonsignificant slower release rates as indicated by greater MDT (**Table 1**) compared with other formulations which contained lower polymer contents.

The prepared formulations were evaluated for drug release kinetics and drug diffusion mechanism. The release kinetics of the optimized as well as tested formulations were best fitted to the Higuchi model suggesting that drug release occurs as a diffusion controlled process based on the Fick's Law where the diffusion coefficient depends upon both the concentration and the time. Bacause the release exponent value of n for the release profiles of all formulations ranged between 0.45 and 0.89, the release mechanism is assumed to follow case II mechanism where both relaxation of the polymer and diffusion of the drug may be involved[65,66].

As shown in **Fig. 9**, non-targeted PEGylated nanomicelles was significantly ($P < 0.05$) more effective than free drug especially on HT-29 cell line. This might be due to the presence of PEG on the surface of nanomicelles. In aqueous environment PEG is highly hydrated and can form a brush-like shell that stretches away from the core. This characteristic prevents the micelle

interaction with adjacent micelles and protein adsorption (opsonization) to the surface of polymeric micelles, which reduces micelle aggregations and their uptake by the mononuclear phagocytic system[42,48,67].

Our results confirm that drug-loaded PLGA-PEG-RA nanomicelles were the most cytotoxic amongst all study groups at all drug concentrations examined. This could be attributed to the receptor-mediated endocytosis mechanism in the cells as well as the nucleus-directed drug release resulting in higher cytotoxicity as oppose to simple endocytosis mechanism, which likely induces lower cytotoxicity[68].

CONCLUSION

PLGA-PEG-RA nanomicelles with low CMC, small size, and appropriate ZP, EE, and release characteristics prepared in the current study present an excellent candidate for the delivery of irinotecan to cancer cells. This PEGylated nanoparticle delivery system well avoids uptake by the reticuloendothelial system, thus improving drug delivery. The incorporation of RA in to the polymer produced significantly higher cell toxicity against cancer cells. Our results imply that the RA-conjugated nanomicelles could have a great potential for targeted therapy and may reduce dose of irinotecan required for therapeutic effects and consequently the adverse effects of this drug.

ACKNOWLEDGEMENTS

The content of this paper is extracted from the Pharm.D thesis No. 391408 submitted by Parnian Maghzi which was financially supported by the Research Department of Isfahan University of Medical Sciences, Isfahan, I.R. Iran

DECLARATION OF INTEREST

We wish to thank the Vice Chancellery of Isfahan University of Medical Sciences for financial support of this work. The authors alone are responsible for the content and writing of the paper.

REFERENCES

1. Ojima I. Guided molecular missiles for tumor-targeting chemotherapy: Case studies using the 2nd-generation taxoids as warheads. ACC Chem. 2008;41:108-119.

2. Kaparissides C, Alexandridou S, Kotti K, Chaitidou S. Recent advances in novel drug delivery systems. J Nano Tech. 2006;2:1-11.

3. Wamoto, T. Clinical application of drug delivery systems in cancer chemotherapy: review of the efficacy and side effect of approved drugs. Biol Pharm Bull. 2013;36(5):715-718.

4. Torchilin VP. Passive and active drug targeting: drug delivery to tumors as an example. Handb Exp Pharmacol. 2010;197:3-53.

5. Kudgus RA, Walden CA, McGovern RM, Reid JM, Robertson JD, Mukherjee P. Tuning pharmacokinetics and biodistribution of a targeted drug delivery system through incorporation of a passive targeting compound. Sci Rep. 2014;4: Article number 5669.

6. Kwon GS. Polymeric micelles for delivery of poorly water-soluble compounds. Crit Rev Ther Drug Carrier Syst. 2003;20:357-403.

7. Yoo HS, Park TG. Folate receptor targeted biodegradable polymeric doxorubicin micelles. J Control Release. 2004;96:273-283.

8. Cheng J, Teply BA, Sherifi I, Sung J, Luther G, Gu FX, Levy-Nissenbaum E, Radovic-Moreno AF, Langer R, Farokhzad OC. Formulation of functionalized PLGA–PEG nanoparticles for in-vivo targeted drug delivery. Biomaterials. 2007;28:869-876.

9. Esmaeili F, Ghahremani MH, Ostad SN, Atyabi F, Seyedabadi M, Malekshahi MR, Amini M, Dinarvand R. Folate-receptor- targeted delivery of docetaxel nanoparticles prepared by PLGA-PEG-folate conjugate. J Drug Target. 2008;16:415-423.

10. Prajna Mishra, Bismita Nayak, RK Dey. PEGylation in anticancer therapy: An overview. Asian J Pharm Sci. 2016,11:337-348.

11. Sadzuka Y, Hirotsu S, Hirota S. Effective irinotecan (CPT-11)-containing liposomes: Intraliposomal conversion to the active metabolite SN-38. Jpn J Cancer Res. 1999;90:226–232.

12. Yarmolenko PS, Zhao Y, Landon C, et al. Comparative effects of thermo sensitive doxorubicin-containing liposomes and hyperthermia in human and murine tumors. Int J Hyperthermia. 2010;26:485-498.

13. Zwicke GL, Mansoori GA, Jeffery CJ. Utilizing the folate receptor for active targeting of cancer nanotherapeutics. Nano Rev. 2012;3:10.3402/nano.v3i0.18496.

14. Tortorella S, Karagiannis TC. Transferrin receptor-mediated endocytosis: a useful target for cancer therapy. J Membr Biol. 2014;247(4):291-307.

15. Varshosaz J, Hassanzadeh F, Sadeghi H, Ghelich Khan Z, Rostami M. Retinoic acid decorated albumin-chitosan nanoparticle for targeted delivery of doxorubicin hydrochloride in hepatocellular carcinoma. J Nanomater. 2013. Doi: Org/10.1155/2013/254157.

16. Siddikuzzaman , Guruvayoorappan C, Berlin Grace VM. All-trans retinoic acid and cancer. Immunopharmacol immunotoxicol. 2011;33(2):241-249.

17. Hong WK, Sporn MB. Recent advances in chemoprevention of cancer. Science. 1997; 278(5340):1073-1077.

18. Nason-Burchenal K, Dmitrovsky E. The retinoids: Cancer therapy and prevention mechanisms. In: Nau H, Blaner W (eds) Retinoids, the biochemical and molecular basis of vitamin A and retinoid action. Handb Exp Pharmacol. Springer, Berlin, 1999;139, PP 301-322.

19. Adamson PC. All-trans-retinoic acid pharmacology and its impact on the treatment of acute promyelocytic leukemia .The Oncologist. 1996;1(5):305-314.

20. Miller WH Jr. The emerging role of retinoids and retinoic acid metabolism blocking agents in the treatment of cancer. Cancer. 1998;83(8):1471-1482.

21. Brtko J, Thalhamer J. Renaissance of the biologically active vitamin A derivatives: established and novel directed therapies for cancer and chemoprevention. Curr Pharm Res. 2003; 9(25):2067- 2077.

22. de The H, Chomienne C, Lanotte M, Degos L, Dejean A. The t(15;17) translocation of acute promyelocytic leukaemia fuses the retinoic acid receptor alpha gene to a novel transcribed locus. Nature.1990;347:558-561.

23. Bukhari MH, Qureshi SS, Niazi S, Asef M, Naheed M, Khan SA, Chaudhry NA, Tayyab M, Hasan M. Chemotherapeutic/chemopreventive role of retinoids in chemically induced skin carcinogenesis in albino mice. Int J Dermatol. 2007;46:1160-1165.

24. Huang M, Ye Y, Chen S, Chai J, Lu J, Zhoa L, Gu L, Wang Z . Use of all-trans retinoic acid in the treatment of acute promyelocytic leukemia. Blood. 1988;72(2):567–572.

25. Kawaguchi R, Zhong M, Kassai M, Ter-Stepanian M, Sun H. Vitamin A transport mechanism of the multitransmembrane, cell-surface receptor STRA6. Membranes. 2015;5:425-453.

26. Berry DC, Levi L, Noy N. Holo-retinol-binding protein and its receptor STRA6 drive oncogenic transformation. Cancer Res. 2014;74(21):6341–6351.

27. Szeto W, Jiang W, Tice DA, Rubinfeld B, Hollingshead PG, Fong SE, Dugger DL, Pham T, Yansura DG, Wong TA, Grimaldi JC, Corpuz RT, Singh JS, Frantz GD, Devaux B, Crowley CW, Schwall RH, Eberhard DA, Rastelli L, Polakis P, Pennica D. Overexpression of the retinoic acid-responsive gene STRA6 in human cancers and its synergistic induction by wnt-1 and retinoic acid. Cancer Res. 2001;61(10):4197–4205.

28. Sun R, Liu Y, Li SY, Shen S, Du XJ, Xu CF, Cao ZT, Bao Y, Zhu YH, Li YP, Yang XZ, Wang J. Co-delivery of all-trans-retinoic acid and doxorubicin for cancer therapy with synergistic inhibition of cancer stem cells. Biomaterials. 2015;37:405-414.

29. Hsiang YH, Wu HY, Liu LF. Topoisomerases: novel therapeutic targets in cancer chemotherapy. Biochem Pharmacol. 1988;37(9):1801-1802.

30. Hsiang YH, Lihou MG, Liu LF. Arrest of replication forks by drug-stabilized topoisomerase I-DNA cleavable complexes as a mechanism of cell killing by camptothecin. Cancer Res. 1989;49(18):5077–5082.

31. Potmesil M. Camptothecins: from bench research to hospital wards. Cancer Res. 1994;54(6):1431–1439.

32. Fuchs C, Mitchell EP, Hoff PM. Irinotecan in the treatment of colorectal cancer. Cancer Treat Rev. 2006;32(7):491-503.

33. Green MR, Harper M, Safa A, Sherman CA, Mushtaq CM, Bahadori H, Brescia FJ, Rocha Lima CM. Irinotecan in the management of patients with pancreatic cancer. Oncology (Williston Park). 2000 ;14(12 Suppl 14):31-33.

34. Gershenson DM. Irinotecan in epithelial ovarian cancer. Oncology (Williston Park). 2002;16(5 Suppl 5):29-31.

35. Vredenburgh JJ, Desjardins A, Reardon DA, Friedman HS. Experience with irinotecan for the treatment of malignant glioma. Neuro Oncol. 2009;11(1):80-91.

36. Boige V, Taïeb J, Hebbar M, Malka D, Debaere T, Hannoun L, Magherini E, Mignard D, Poynard T, Ducreux M. Irinotecan as first-line chemotherapy in patients with advanced hepatocellular carcinoma: a multicenter phase II study with dose adjustment according to baseline serum bilirubin level. Eur J Cancer. 2006;42(4):456-9.

37. Xu Z, Shao J, Li L, Peng X, Chen M, Li G, Yan H, Yang B, Luo P, He Q. All-trans retinoic acid synergizes with topotecan to suppress AML cells via promoting RARα-mediated DNA damage. BMC Cancer. 2016;16:2. DOI: 10.1186/s12885-015-2010-6.

38. Ramesh M, Ahlawat P, Srinivas NR. Irinotecan and its active metabolite, SN-38: review of bioanalytical methods and recent update from clinical pharmacology perspectives. Biomed Chromatogr. 2010;24(1):104-123.

39. Akimoto K, Kawai A, Ohya K. Kinetic studies of the hydrolysis and lactonization of camptothecin and its derivatives, CPT-11 and SN-38, in aqueous solution. Chem Pharm Bull. 1994;42:2135-8.

40. Garcia-Carbonero R, Supko JG. Current perspectives on the clinical experience, pharmacology, and continued development of the camptothecins. Clin Cancer Res. 2002;8:641-61.

41. Vanhoefer U, Harstrick A, Achterrath W, Cao S, Seeber S, Rustum YM. Irinotecan in the treatment of colorectal cancer: clinical overview. J Clin Oncol. 2001;19:1501-1518.

42. Zhang Z, Yao J. Preparation of irinotecan-loaded folate-targeted liposome for tumor targeting delivery and its antitumor activity. AAPS Pharm Sci Tech. 2012;13(3),802-810.

43. Zhang L, Cao D-Y, Wang J, Xiang B, Dun J-N. PEG-coated irinotecan cationic liposomes improve the therapeutic efficacy of breast cancer in animals. Eur Rev Med Pharmocol Sci. 2013; 17:3347-3361.

44 Tochilin VP. Structure and design of polymeric surfactant-based drug delivery systems. J Control Release. 2001;56(3):337-346.

45. Zhou J, Romero G, Rojas E, Moya S, Ma L, Gao C. Folic acid modified poly(lactide-co-Glycolide) nanoparticles, layer-by-layer surface engineered for targeted delivery. Macromol Chem Phys. 2010;211:404-411

46. Saxena V, Naguib Y, Delwar Hussain M. Folate receptor targeted 17-allylamino-17-demethoxygeldanamycin (17-aag) loaded polymeric nanoparticles for breast cancer. Colloid Surface B. 2012;94:274-280.

47. Hami Z, Amini M, Ghazi-Khansari M, Rezayat SM, Gilani K. Doxorubicin-conjugated PLA-PEG-Folate based polymeric micelle for tumor-targeted delivery: synthesis and in vitro evaluation. Daru. 2014;22(1):30. doi: 10.1186/2008-2231-22-30.

48. Boddu Sai HS, Vaishya R, Jwala J, Vadlapudi A, Pal D, Mitra AK. Preparation and characterization of folate conjugated nanoparticles of doxorubicin using PLGA-PEG-FOL Polymer. Med Chem. 2012;2(4):068-075.

49. Emami J, Rezazadeh M, Rostami M, Hassanzadeh F, Sadeghi H, Mostafavi A, Minaiyan M, Lavasanifar A. Co-delivery of paclitaxel and α-tocopherol succinate by novel chitosan-based polymeric micelles for improving micellar stability and efficacious combination therapy. Drug Dev Ind Pharm. 2015;41(7):1137-1147.

50. Rezazadeh M, Emami J, Hasanzadeh F, Sadeghi H, Minaiyan M, Mostafavi A, Rostami M, Lavasanifar A. In vivo pharmacokinetics, biodistribution and anti-tumor effect of paclitaxel-loaded targeted chitosan-based polymeric micelle. Drug Deliv. 2016;23(5):1707-1717.

51. Emami J, Pourmashhadi A, Sadeghi H, Varshosaz J, Hamishehkar H. Formulation and optimization of celecoxib-loaded PLGA nanoparticles by the Taguchi design and their in vitro cytotoxicity for lung cancer therapy. Pharm Dev Technol. 2015;20(7):791–800.

52. Sharma S, Sharma MC. Development and validation of Spectrophotometric method and TLC densitometric determination of irinotecan HCl in pharmaceutical dosage forms. Arabian J of Chem. 2016;9(2):S1368–S1372.

53. Jindal N, Mehta SK. Nevirapine loaded poloxamer/pluronic P123 mixed micelles: optimization of formulation and in vitro evaluation. Colloid Surface B. 2015;129:100-106.

54. Costa P, Lobo JMS. Modeling and comparison of dissolution profiles. Eur J Pharm Sci. 2001;13:123-133.

55. Emami J, Rezazade M, Varshosaz J, Tabbakhian M, Aslani A. Formulation of LDL targeted nanostructured lipid carrier loaded paclitaxel; a detailed of preparation, freeze drying condition, and in vitro cytotoxicity. J Nanomaterial. 2012; Article ID 358782, doi:10.1155/2012/358782.

56. Ebrahimnejad P, Dinarvand R, Sajadi A, Jaafari MR, Nomani AR, Azizi E, Rad-Malekshahi M, Atyabi F. Preparation and in vitro evaluation of actively targetable nanoparticles for SN-38 delivery against HT-29 cell lines. Nanomedicine. 2010;6(3):478-485.

57. Sai HS, Boddu R, Vaishya J, Jwala A, Vadlapudi D, Pal A, Mitra K. Preparation and characterization of folate conjugated nanoparticles of doxorubicin using PLGA-PEG-FOL polymer. Med chem. 2012;2(4):068-075.

58. Nagarwal RC, Kant S, Singh PN, Maiti P, Pandit JK. Polymeric nanoparticulate system: a potential approach for ocular drug delivery. J Control Release. 2009;136(1):2-13.

59. Allen TM, Cullis PR. Drug delivery systems: Entering the mainstream. Science. 2004;303: 1818-1822.

60. Hami Z, Amini M, Ghazi-Khansari M, Rezayat SM, Gilani K. Doxorubicin-conjugated PLA-PEG-Folate based polymeric micelle for tumor-targeted delivery: Synthesis and *in vitro* evaluation. DARU J Pharm Sci. 2014,22:30,1-7.

61. Hobbs SK, Monsky WL, Yuan F, Roberts WG, Griffith L, Torchilin VP, Jain RK. Regulation of transport pathways in tumor vessels: role of tumor type and microenvironment. Proc Natl Acad Sci .1998;95:4607-4612.

62. Kim K, Kwon S, Hyung PJ, Chung H, Young JS. Physicochemical characteristics of self-assembled nanoparticles based on glycol chitosan bearing 5β-cholanic acid. Langmuir. 2003;19:10188–10193.

63. Wang F, Chen Y, Zhang D, Zhang Q, Zheng D, Hao L, Liu Y, Duan C, Jia L, Liu G. Folate-mediated targeted and intracellular delivery of paclitaxel using a novel deoxycholic acid-*O*-carboxymethylated chitosan–folic acid micelles. Int J Nanomed. 2012;7:325-337.

64. Robert J, Rivory L. Pharmacology of irinotecan. Drugs Today (Barc). 1998;34(9):777-803.
65. Ritger PL, Peppas NA. A simple equation for description of solute release I. Fickian and non-Fickian release from non-swellable devices in the form of slabs, spheres, cylinders or discs. J Control Release. 1987;5:23-36.
66. Peppas NA, Sahlin JJ. A simple equation for the description of solute release. III. Coupling of diffusion and relaxation. Int J Pharm. 1989;57(2):169-172.
67. Li W, Zhana P, Clercqb ED, Loua H, Liua X. Current drug research on PEGylation with small molecular agents. Prog Pol Sci. 2013;38:421-444.
68. Mahalwara A, Sharmaa A, Sahub R. Evaluation of receptor mediated endocytosis on cellular internalization: a comparative study of pegylated nanoparticles and folate anchored pegylated nanoparticles on mda-mb-231 cells. Int J Biol Pharm Res. 2012;3(3):431-443.

Table and Figure titles

Table 1. Composition of different formulations of irinotecan-loaded-PLGA-PEG-RA micelles generated by an L4 orthogonal array using Taguchi design and their Physical characteristics.

Table 2. Predicted *vs* actual responses obtained for the optimized (F_2) formulation.

Table 3. IC_{50} values (µg/mL) of different formulations after 72 h exposure to HT-29 and HepG cell lines.

Fig. 1. Synthesis schemes of (a), poly (lactic-co-glycolic acid)-polyethylene glycol (PLGA-PEG); and (b), poly (lactic-co-glycolic acid)-polyethylene glycol-retinoic acid (PLGA-PEG-RA).

Fig. 2. ^{1}H-NMR spectrum of (A), poly (lactic-co-glycolic acid) (PLGA); (B), polyethylene glycol (PEG) bis(amine).

Fig. 3. ^{1}H-NMR spectrum of (A), retinoic acid (RA); (B) poly (lactic-co-glycolic acid)-polyethylene glycol-retinoic acid (PLGA-PEG-RA).

Fig. 4. ^{1}H-NMR spectrum of physical mixture of poly (lactic-co-glycolic acid) (PLGA), polyethylene glycol (PEG), and retinoic acid (RA).

Fig. 5. FTIR Spectra of (a), polyethylene glycol (PEG) bis(amine); (b), poly (lactic-co-glycolic acid) (PLGA); (c), retinoic acid (RA); (d), poly (lactic-co-glycolic acid)-polyethylene glycol-retinoic acid (PLGA-PEG-RA).

Fig. 6. Contribution percent of different factors on the particle size, zeta potential, entrapment efficiency, and mean release time of nanomicelles loaded with irinotecan.

Fig. 7. Transmission electron microscope photograph of poly (lactic-co-glycolic acid)-polyethylene glycol-retinoic acid (PLGA-PEG-RA) micelles. Inset image shows a magnified nanoparticle with increasing resolution and details.

Fig. 8. *In vitro* drug release profiles from poly (lactic-co-glycolic acid)-polyethylene glycol-retinoic acid (PLGA-PEG-RA) micelles. Data were plotted as Mean ± SD.

Fig. 9. *In vitro* cytotoxicity of different formulations and blank micelles against (A) HT-29 and (B) HepG2 cell lines. Data are presented as Mean ± SD.

a

PEG-(bis-amine)
Mw=2000

PLGA(50:50)
Mw=12000

DCC/NHS

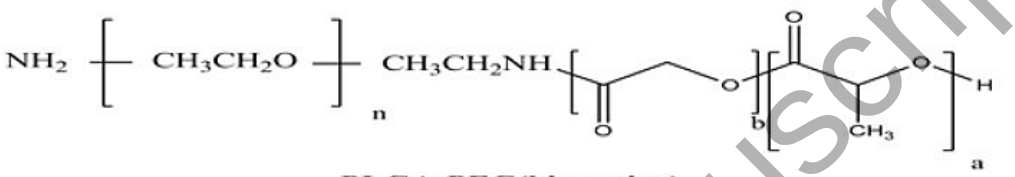

PLGA-PEG(bis-amine)

b

Retinoic acid
Mw=300.435

PLGA-PEG(bis-amine)

DCC/NHS

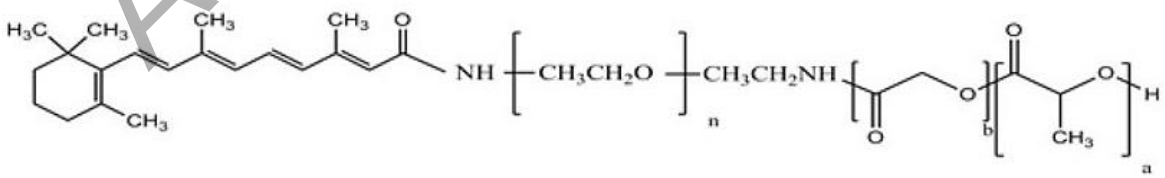

PLGA-PEG(bis-amine)-Retinoic acid

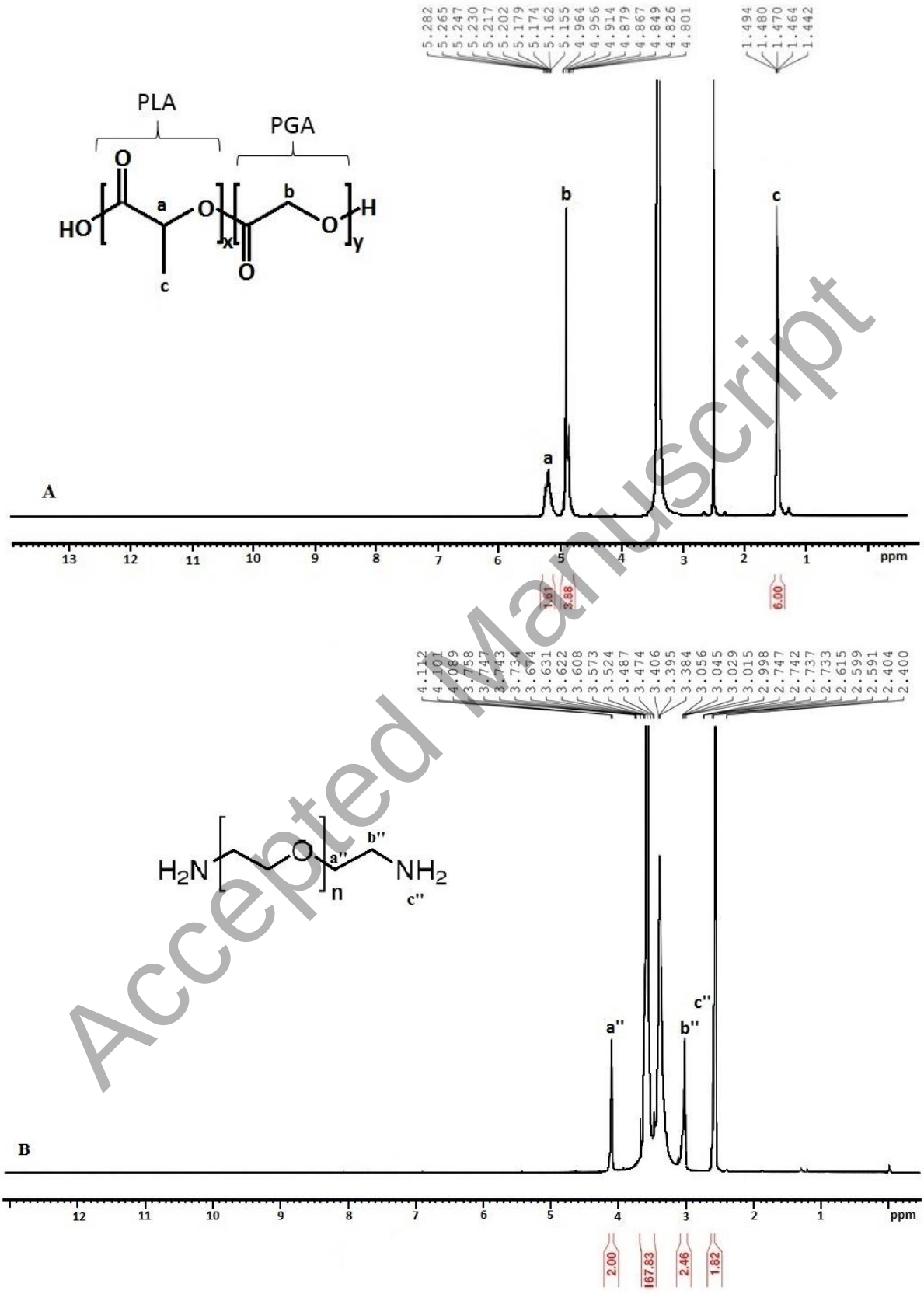

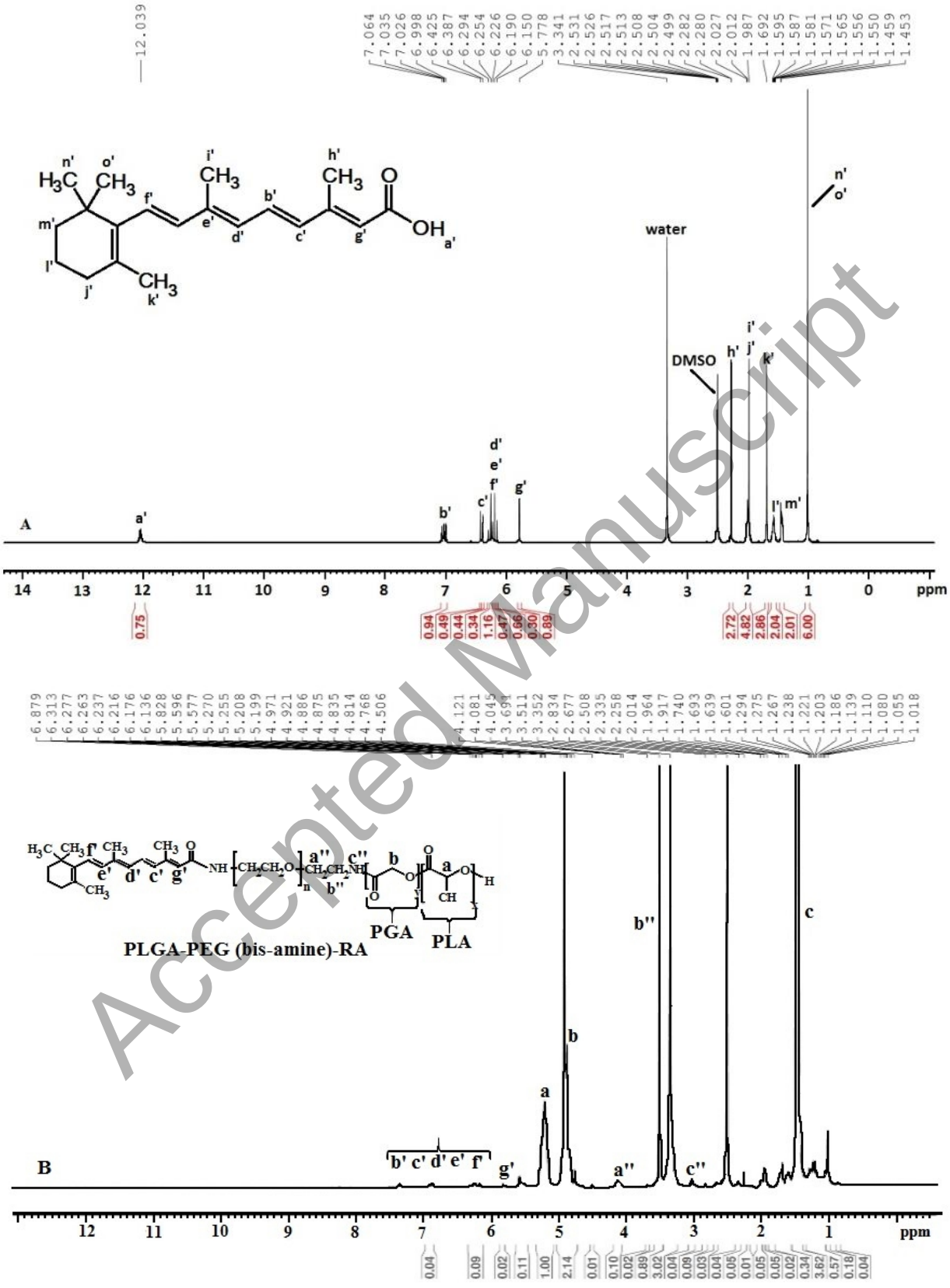

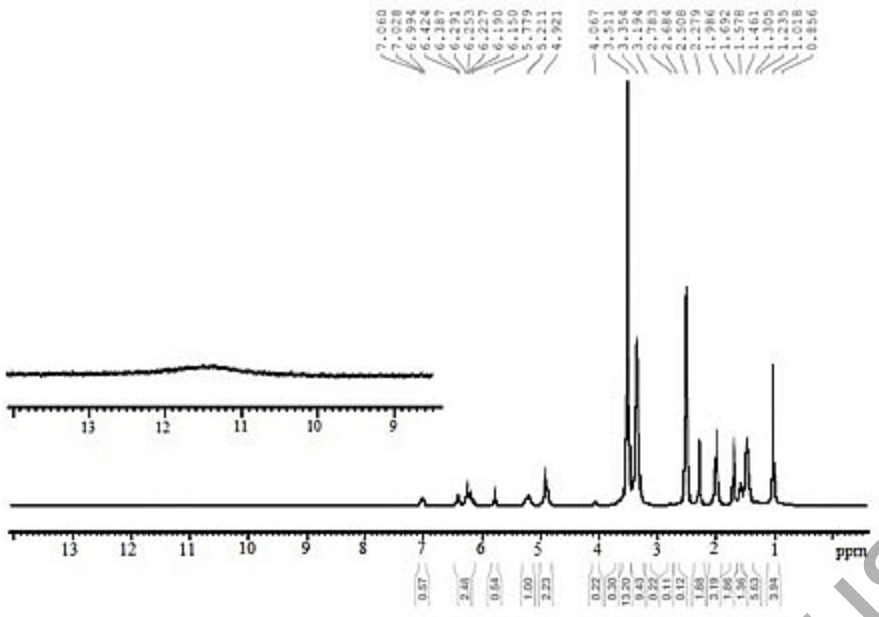

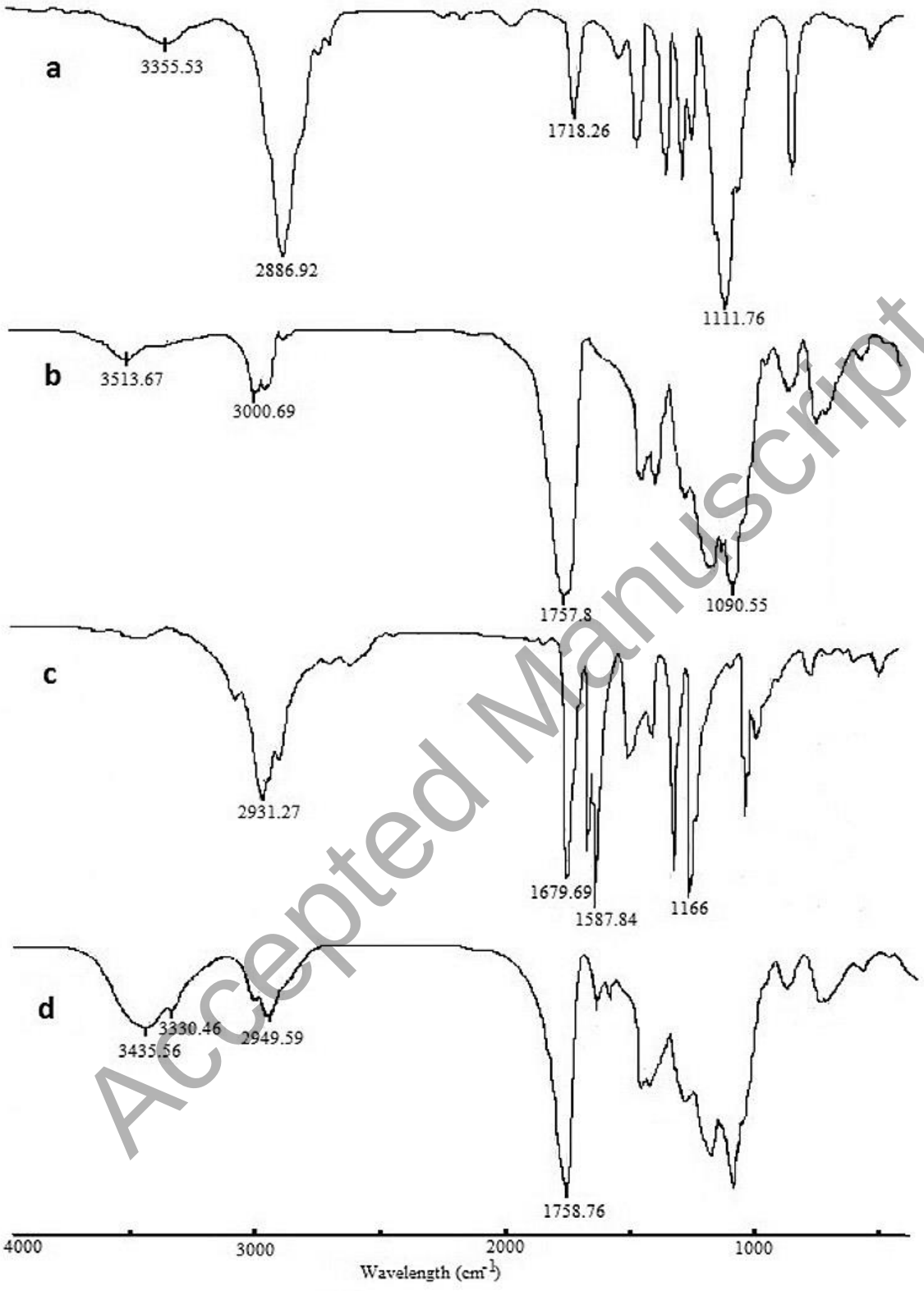

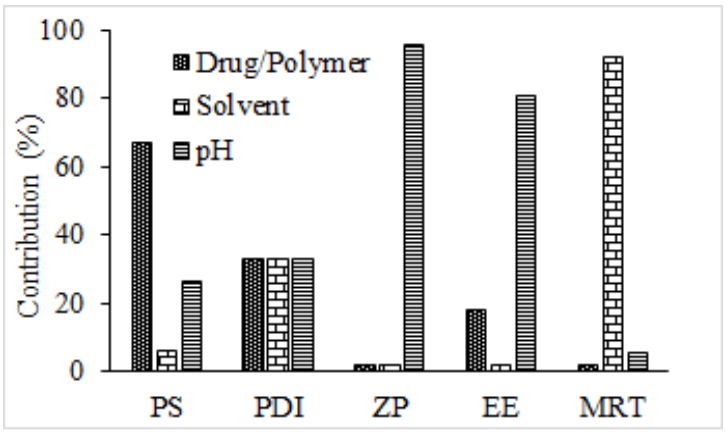

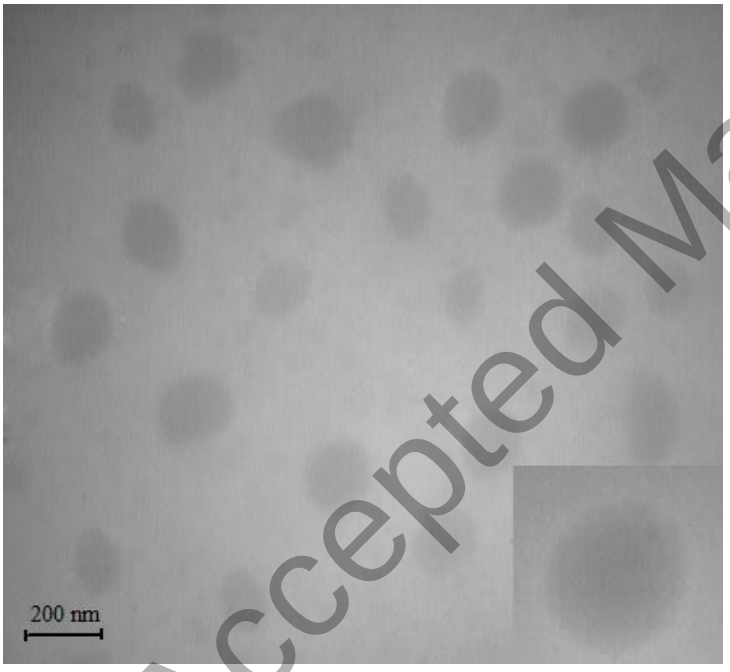

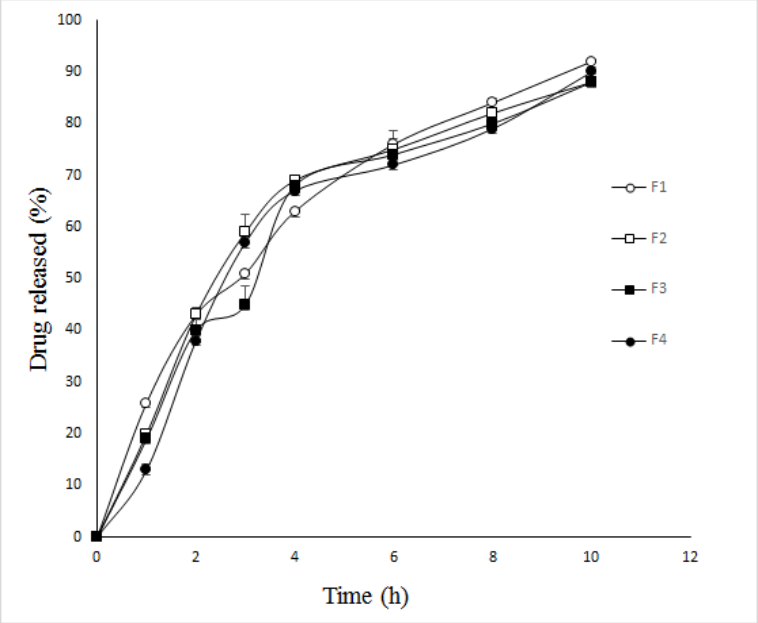

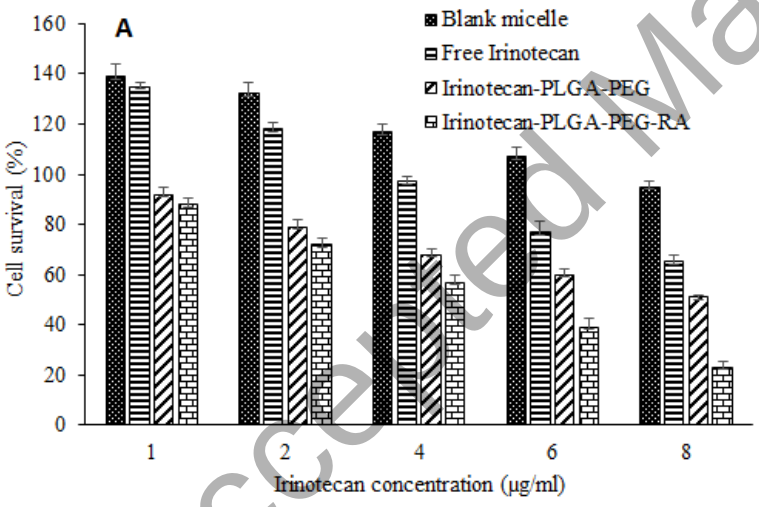

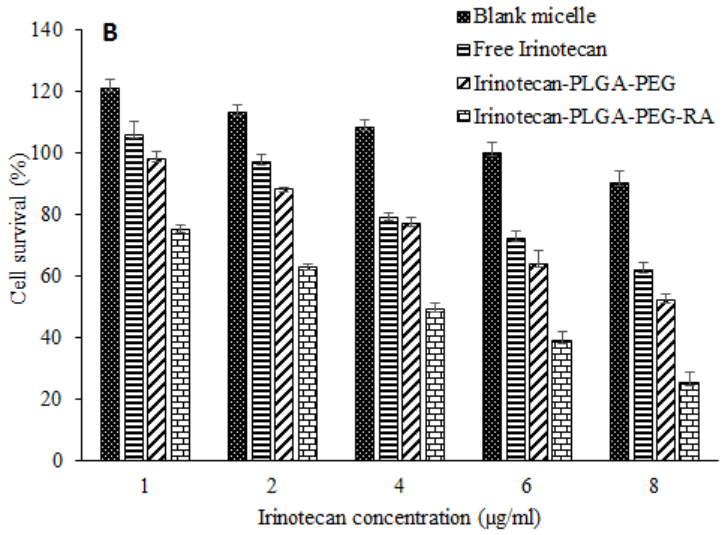

Table 1.

F	D/P	A/E	pH	PS (nm)	PDI	ZP (mV)	EE (%)	MRT (h)	n
F1	1:5	1:1	9	174 ± 5.81	0.26 ± 0.07	-20.3 ± 0.51	81.3 ± 4.02	3.33 ± 0.64	0.666
F2	1:2.5	1:1	7	160 ± 9.31	0.22 ± 0.06	-24.0 ± 4.03	83.2 ± 3.61	3.43 ± 0.35	0.711
F3	1:2.5	1.5:0.5	9	148 ± 10.5	0.23 ± 0.05	-20.0 ± 1.72	79.3 ± 6.61	3.15 ± 0.46	0.773
F4	1:5	1.5:0.5	7	209 ± 14.0	0.36 ± 0.11	-23.6 ± 3.01	84.6 ± 2.53	3.31 ± 0.13	0.875

F, Formulation; D/P, Drug/Polymer; A/E, Acetone/Ethanol; pH, Potential of Hydrogen; PS, Particle Size; PDI, Polydispersity Index; ZP, Zeta Potential; EE, Entrapment Efficiency; n, Release Exponent.

Table 2.

Responses	PS (nm)	PDI	ZP (mV)	EE (%)	MRT (h)
Actual	160 ± 9.13	0.20 ± 0.05	-24.9 ± 4.03	83.9 ± 3.61 0.51	3.28 ± 0.35
Predicted	159	0.22	-24.1	83.1	3.19
Error (%)	0.62	10	3.21	0.95	2.74

PS, Particle Size; PDI, Polydispersity Index; ZP, Zeta Potential; EE, Entrapment Efficiency.

Table 3.

Drug formulation	HT-29	HepG2
Free irinotecan	9.0 ± 0.15	9.5 ± 0.23
Irinotecan-loaded PLGA-PEG	7.8 ± 0.21*	8.2 ± 0.19
Irinotecan-loaded PLGA-PEG-RA	4.2 ± 0.11*	4.8 ± 0.13*